

Evaluation of Excess Interstitial Silicon Amount Using Delta-doped Boron Markers Grown by UHV-CVD

Masayuki Hiroi, Takeo Ikezawa, Masami Hane, and Akio Furukawa

*Silicon Systems Research Laboratories, NEC Corporation,
1120 Shimokuzawa, Sagami-hara, 229-1198, Japan*

Tel: +81-42-771-0797, Fax: +81-42-771-0886, E-mail: hiroi@mel.cl.nec.co.jp

Abstract- Interstitial-silicon emission from {311} defects during postannealing after Si self-implantation was investigated using boron delta-doped marker layers epitaxially grown by ultrahigh-vacuum chemical vapor deposition. The amount of excess interstitials which remain after interstitial-vacancy recombination at early stage of postannealing after various implantation conditions was also evaluated. The amount of excess interstitials was nearly independent of implantation dose and energy, but greatly depended on implant species. A larger number of interstitials was found for implantation of arsenic than for implantation of silicon or boron.

INTRODUCTION

Transient enhanced diffusion (TED) during annealing just after ion implantation has been an important phenomenon limiting how shallow we can make p-n junctions, which need to be shallower for scaled CMOS. Simulations of TED in silicon (Si) have been greatly advanced by taking account of the kinetics between excess interstitial silicon and {311} defects[1]. The excess interstitials, which cause TED, are much smaller than the ones before the postannealing, since most of implantation-induced interstitials and vacancies recombine at early stage of the annealing. The "+1" model[2] has been widely used for the initial condition of the interstitial silicon atoms in the TED simulation. This model assumes perfect recombination of a large number of the implantation-induced point defects, and provides the same amount of remaining interstitials as implanted ions independently of ion species. However, some recent experimental results[4,5] indicate that the 'effective' amount of excess interstitial silicon after the recombination should increase with increasing ion mass.

In this paper, we estimated the interstitial emission from {311} defects during TED using boron (B) delta-doped superlattices grown by an ultrahigh-vacuum chemical vapor deposition (UHV-CVD). The effective amount of excess interstitial silicon was also calculated from experimental data obtained during long-term annealing.

EXPERIMENT

The B delta-doped superlattices were grown on Si(100) substrates by the UHV-CVD to obtain a low background concentration of carbon (C), which acts as a sink for the interstitials[9], because it is difficult to suppress the C contamination from the e-gun evaporator in conventional Si molecular beam epitaxy.

Five series of the B spike and a 300-nm non-doped layer were epitaxially grown on a 3- μ m-thick

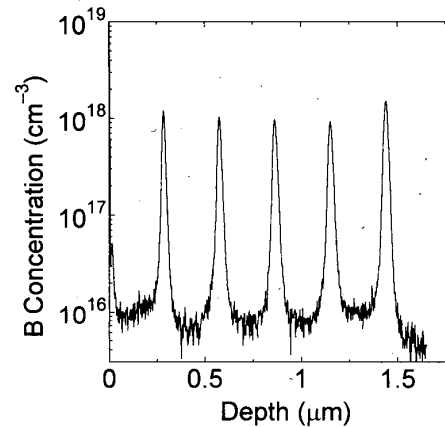


Figure 1: B profile of as-grown sample.

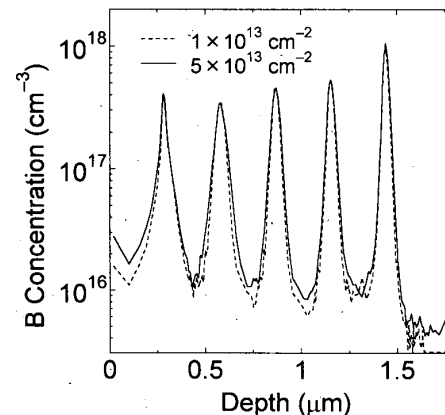


Figure 2: B profiles of Si 40 keV, 1 and 5×10^{13} cm^{-2} implantation.

non-doped buffer layer, as shown in Fig. 1. Defects were introduced to the sample by Si self-implantation at 40 keV at a dose of $1-5 \times 10^{13} \text{ cm}^{-2}$ in order to study the interstitial emission from the $\{311\}$ defects. The samples were annealed at 600–750°C for the time in which TED was dominated by the $\{311\}$ defect dissolution. The dominance was confirmed by the implantation-dose independent B diffused profiles (Fig. 2). To study the dependence of the effective amount of interstitial silicon on the implanted species, we implanted B, Si, and arsenic (As) at 10–80 keV, $1-5 \times 10^{13} \text{ cm}^{-2}$, and then annealed the samples at 750°C for 120 min.

INTERSTITIAL SILICON EMISSION FROM $\{311\}$ DEFECTS

Relatively deep marker layers, which was avoided from B clustering, were analyzed using the effective B diffusivity,

$$D_B = D_B^* \frac{C_I}{C_I^*}, \quad (1)$$

where C_I is the concentration of free interstitials and the superscript * indicates thermal equilibrium. To simulate the interstitial silicon emission from $\{311\}$ defects, we used the following model[3]:

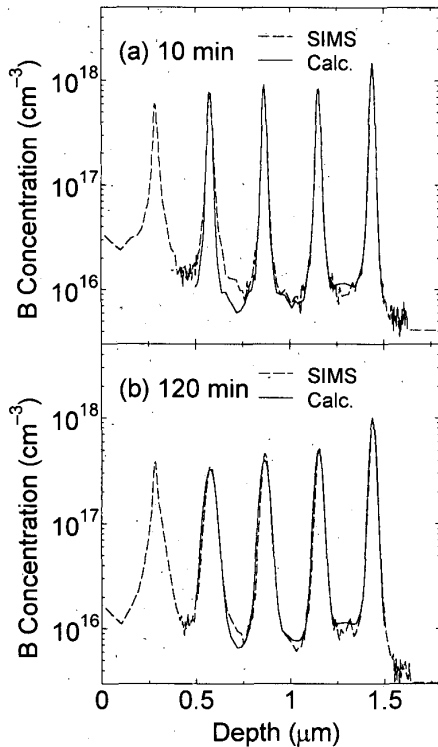


Figure 3: Diffused B profiles of Si 40 keV, $1 \times 10^{13} \text{ cm}^{-2}$ implantation, following annealing at 600° C. Good agreement was obtained by the model of the interstitial emission from the $\{311\}$ defects.

$$\frac{dC_{311}}{dt} = 4\pi\alpha a D_I C_{311} (C_I - C_{I,311}). \quad (2)$$

Here, D_I is the interstitial diffusivity, C_{311} is the concentration of interstitials incorporated in the $\{311\}$ defects, and $C_{I,311}$ is the critical interstitial concentration above which all the interstitials are removed from the free interstitial population to the incorporated one. During the $\{311\}$ defect dissolution, the interstitials are emitted with the transport capacity $D_I C_{I,311}$. The maximum interstitial supersaturation is also written using $D_I C_{I,311}$ as

$$\frac{C_{I,311}}{C_I^*} = \frac{D_I C_{I,311}}{D_I C_I^*}. \quad (3)$$

We fitted the experimentally obtained B

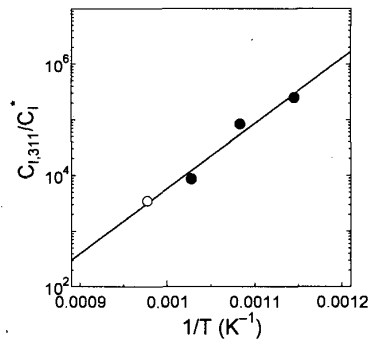


Figure 4: Temperature dependence of enhancement factor.

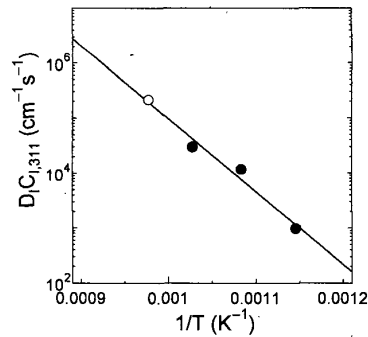


Figure 5: Temperature dependence of interstitial emission rate.

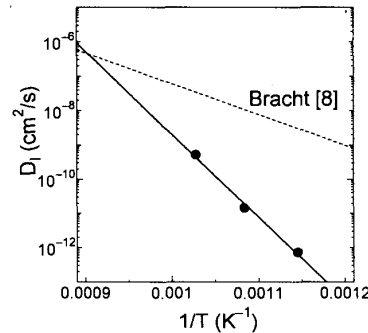


Figure 6: Temperature dependence of interstitial diffusivity.

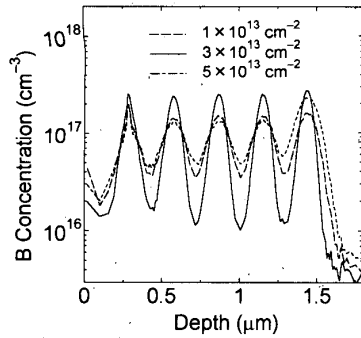


Figure 7: B profiles of As implantation at 40 keV, 1, 3, and $5 \times 10^{13} \text{ cm}^{-2}$, following [annealing at?] 750° C for 120 min.

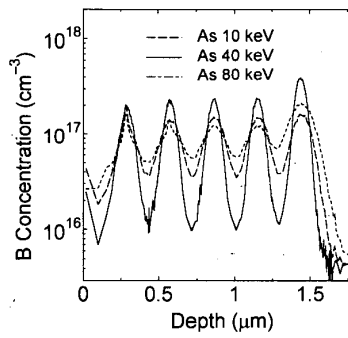


Figure 8: B profiles of As $3 \times 10^{13} \text{ cm}^{-2}$ implantation at 10, 40, and 80 keV, following [annealing at?] 750° C for 120 min.

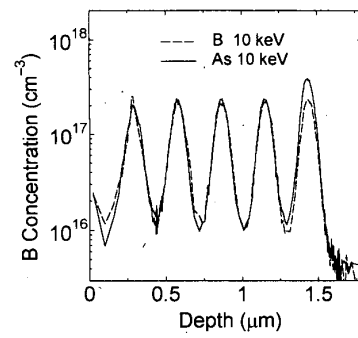


Figure 9: B profiles of B, As $3 \times 10^{13} \text{ cm}^{-2}$ implantation, following [annealing at?] 750° C for 120 min.

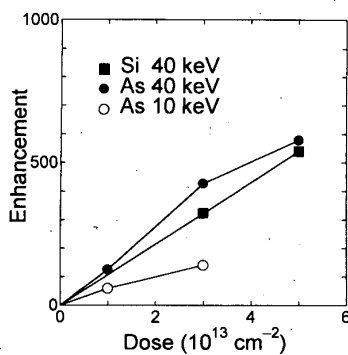


Figure 10: Dose dependence of time-averaged enhancement during [annealing at?] 750° C for 120 min.

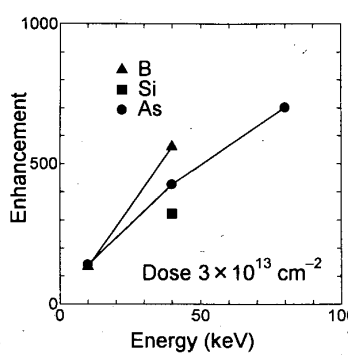


Figure 11: Energy dependence of time-averaged enhancement during [annealing at?] 750° C for 120 min.

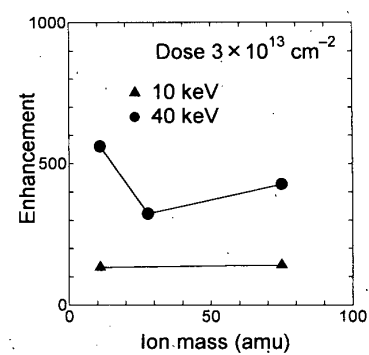


Figure 12: Ion mass dependence of time-averaged enhancement during [annealing at?] 750° C for 120 min.

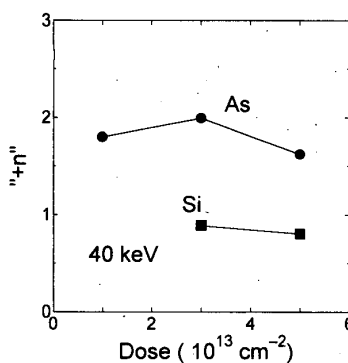


Figure 13: Dose dependence of "+n".

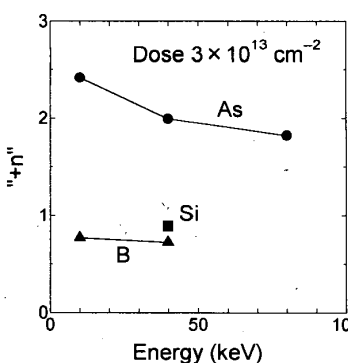


Figure 14: Energy dependence of "+n".

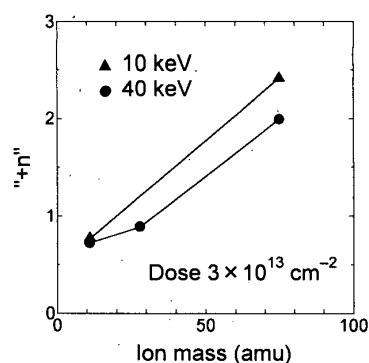


Figure 15: Ion mass dependence of "+n".

diffused profiles with these two parameters, D_1 and $C_{1,311}$ (Fig. 3). The C_1^* was derived as $(D_1 C_1^*)/D_1$, because various values of D_1 and C_1^* have been reported; their products $D_1 C_1^*$, however, are nearly the same[6].

The values of $C_{1,311}/C_1^*$ and $D_1 C_{1,311}$ obtained by the fitting are shown in Figs. 4 and 5. The data for relatively long annealing during TED could be used to evaluate $C_{1,311}/C_1^*$, since C_1 almost reaches $C_{1,311}$. In this case the observed enhancement-factor C_1/C_1^* would be nearly the same as $C_{1,311}/C_1^*$ throughout the analyzed region. The values of $D_1 C_{1,311}$ can be reduced from those of $C_{1,311}/C_1^*$ by the relation described above.

In contrast to the evaluation of $D_1 C_{1,311}$, D_1 had to be estimated from the data for relatively short annealing, because D_1 can be reduced just from depth dependence, and depth dependence becomes smaller as annealing time is increased. According to the $D_1 C_{1,311}$ values, the D_1 values, which reproduce well the experimentally obtained B diffused profiles of the short annealing, were estimated to be lower than the ones obtained from metal diffusion data[8](Fig. 6). We think that the difference is due to the initial rapid TED[10], which is caused by the interstitials escaping from the {311} defect formation. The larger C_1 at the very early stage of annealing produces greater depth-dependence, which gives a smaller D_1 and a larger $C_{1,311}$ in the estimation from a fixed $D_1 C_{1,311}$ than that of TED dominated by the {311} defects dissolution.

DEPENDENCE OF EXCESS INTERSTITIAL SILICON AMOUNT ON IMPLANTATION CONDITION

The effective amount of the excess interstitials was evaluated from the B marker diffusion during relatively high-temperature and long annealing (750° C, 120 min), which completely dissolves {311} defects[5]. Figures 7-9 show the diffused B profiles, and Figs. 10-12 show the time-averaged enhancement of those samples.

The dependence of the B diffusion enhancement during the annealing on the implantation conditions agrees with previous reports[5]. The enhancement (i) was nearly proportional to the dose (Figs. 7, 10), (ii) increased with increasing implantation energy (Figs. 8, 11), and (iii) was practically independent of the ion species (Fig. 9, 12). These results imply that As implantation produces more TED than B implantation does when the implanted ranges are the same, because the energy must be higher for As than for B. This contradicts the "+1" model, which gives the same profiles for the interstitials as for the implanted ions.

We derived effective plus factor "+n", which

is the ratio to the "+1" model, from the experimentally obtained diffused profiles. The +n value was nearly independent of the dose (Fig. 13) and the energy, but slightly increased when the implantation range became much smaller (Fig. 14). The values for As are 2-3 times those for B (Fig. 15). This dependence on the implantation condition agrees with that obtained by the calculation using Monte Carlo simulation of ion implantation [7], and can be explained by displacement between interstitial and vacancy profiles [7].

SUMMARY

Using epitaxially grown delta-doped B superlattices, we evaluated interstitial silicon emission from {311} defects and the effective amount of excess interstitials. Thanks to the deep marker structures, the evaluation could be carried out using a simple assumption of enhanced B diffusivity without B clustering. The results show that a larger number of interstitials were produced by As implantation than by B or Si implantation.

ACKNOWLEDGEMENTS

We would like to thank Drs. H. Abe and T. Kunio for their encouragement. We would also like to thank T. Aoyama for epitaxial growth.

REFERENCES

- [1] J.M. Poate, D.J. Eaglesham, G.H. Gilmer, H.-J. Gossmann, M. Jaraiz, C.S. Rafferty, and P.A. Stolk, *proc. IEDM95*, p. 77 (1995).
- [2] M.D. Giles, *J. Electrochem. Soc.*, **138**, 1160 (1991).
- [3] C.S. Rafferty, G.H. Gilmer, M. Jaraiz, D.J. Eaglesham, and H.-J. Gossmann, *Appl. Phys. Lett.*, **68**, 2395 (1996).
- [4] H.S. Chao, P.B. Griffin, J.D. Plummer and C.S. Rafferty, *Appl. Phys. Lett.*, **69**, 2113 (1996).
- [5] P.B. Griffin, R.F. Lever, R.Y.S. Huang, H.W. Kennel, P.A. Packman, and J.D. Plummer, *proc. IEDM93*, p. 295 (1995).
- [6] L. Pelaz, G.H. Gilmer, M. Jaraiz, S.B. Herner, H.-J. Gossmann, D.J. Eaglesham, G. Hobler, C.S. Rafferty, and J. Barbolla, *Appl. Phys. Lett.*, **73**, 1421 (1998).
- [7] U. Gösele, D. Conrad, P. Werner, Q.-Y. Tong, R. Gafiteanu, and T.Y. Tan., *Mat. Res. Soc. Symp. Proc.*, **469**, p.13 (1997).
- [8] H. Bracht, N.A. Stolwijk, and H. Mehrer, *Mater. Sci. Forum*, **143-147**, 785 (1994).
- [9] P.A. Stolk, H.-J. Gossmann, D.J. Eaglesham, D.C. Jacobson, C.S. Rafferty, G.H. Gilmer, M. Jaraiz, J.M. Poate, H.S. Luftman, and T.E. Haynes, *J. Appl. Phys.*, **81**, 6031 (1997).
- [10] T. Saito, J. Xia, R. Kim, T. Aoki, H. Kobayashi, Y. Kamakura, and K. Taniguchi, *proc. IEDM98*, p. 497 (1998).